

Reanalysis of crystal-field parameters for Nd^{3+} ions in $\text{Nd}_2\text{BaCuO}_5$ and $\text{Nd}_2\text{BaZnO}_5$ based on standardization, multiple correlated fitting technique, and dataset closeness

Czesław Rudowicz,* Paweł Gnutek, and Mirosław Karbowski†

Institute of Physics, Szczecin University of Technology, al. Piastów 17, 70-310 Szczecin, Poland

(Received 13 December 2006; published 27 September 2007)

This paper elucidates some subtle properties of the orthorhombic and monoclinic symmetry crystal-field (CF) Hamiltonians (H_{CF}), which are not fully understood by some authors. These properties bear on interpretation of experimental data obtained in, e.g., optical spectroscopy, inelastic neutron scattering, and magnetic susceptibility measurements. Our reanalysis of CF parameters (CFPs) is based on application of the standardization idea as well as the idea of dataset closeness. The closeness of any two CFP sets may be represented by the closeness factor C and the norm ratio $R=N_A/N_B$ for the respective H_{CF} terms: $k=2, 4, 6$, and the global ones C_{gl} . The specific aims of this paper are twofold. The first aim is to clarify the controversy arising when comparing the standard CF parameters with the nonstandard CFPs. This controversy, originating from the lack of awareness of the standardization applicable to the orthorhombic (as well as monoclinic and triclinic) CFP datasets, is evident, e.g., in the recent study of Nd^{3+} ion in $\text{Nd}_2\text{BaCuO}_5$ by R. S. Puche *et al.* [Phys. Rev. B **71**, 024403 (2005)]. This leads to an unjustified criticism of the data of other authors. Consideration of standardization and dataset closeness also helps in identifying other inconsistencies concerning R. S. Puche *et al.*'s results. The second aim is to determine the alternative physically equivalent CFP datasets generated by the standardization transformation. These CFP datasets are utilized in the multiple correlated fitting technique (MCFT) to improve the reliability of the final fitted CFPs. Additional refittings of the original energy level data are carried out starting from distinct regions in the parameter space. The independently fitted nonstandard CFPs obtained in this way are then transformed to the standard region and intercorrelated. Our considerations enable us to solve the controversy in question and improve the understanding of the intricacies inherent in the low-symmetry CFP datasets. A comparative analysis of the CFPs for various rare earth R^{3+} ions in $R_2\text{BaXO}_5$ ($X=\text{Cu, Zn, Ni, and Co}$), and related crystals will be carried out elsewhere.

DOI: [10.1103/PhysRevB.76.125116](https://doi.org/10.1103/PhysRevB.76.125116)

PACS number(s): 75.10.Dg, 75.30.Gw, 71.70.Ch, 61.66.Fn

I. INTRODUCTION

Standardization^{1,2} has a long tradition in electron magnetic resonance (EMR) studies^{3–6} of transition ions with spin $S \geq 1$, since it originated from analysis of experimental EMR spectra in the 1960s; for earlier references, see Ref. 1. Applications of the orthorhombic¹ and monoclinic² standardization to the zero-field-splitting (ZFS) parameters of rank $k=2, 4$, and 6 for various ion-host systems have been dealt with in Refs. 7 and 8. In crystal-field theory (CFT) and optical spectroscopy studies,^{9–12} standardization has also proved to be valuable.^{13–15} However, in spite of the documented importance,^{7,8,13–15} standardization^{1,2} has not been utilized by some authors, who inadvertently report nonstandard CF parameters (CFPs) or ZFS parameters (ZFSPs) obtained from fitting experimental data.

The major point is that such nonstandard CFPs (Refs. 13–15) or ZFSPs (Refs. 7 and 8) can be directly compared neither with other nonstandard parameters belonging to different regions in the multiparameter space nor with the standard parameters commonly prevailing in the literature. Several papers are published every year reporting CFP (ZFSP) datasets outside the standard range, thus indicating the lack of awareness of the standardization idea by the authors. Any meaningful comparison of such datasets requires that the parameters are expressed in the same region of the multiparameter space. Hence, comparison of numerically distinct yet implicitly physically equivalent CFP datasets, without realization that such datasets must be first transformed into the

same region of the multiparameter space, may lead to serious problems, e.g., confusion, controversy, or even unjustified criticism of the experimental and/or theoretical results of other authors. The fact that, for certain symmetry cases, a number of alternative physically equivalent CFP datasets may be obtained from the least-squares fittings creates an ambiguity and thus complicates the fitting process and interpretation of the results. Importantly, the existence of such correlated fitted CFP datasets may be turned into an advantage. These sets may be utilized to improve the reliability of the final fitted results within the multiple correlated fitting technique (MCFT) originally proposed in Ref. 2 and extended in Ref. 14. Since the application of the MCFT requires access to raw experimental data and several refittings, only one paper¹³ confirming the practical usefulness of the MCFT has appeared so far. Another application of the MCFT is considered in this paper.

A recent example of the problems in question is provided by two nonstandard CFP datasets for the Nd^{3+} ion in $\text{Nd}_2\text{BaCuO}_5$ reported by R. S. Puche *et al.*¹⁶ The semiempirical nonstandard CFPs were subsequently used as the starting parameters for fitting the experimental Nd^{3+} energy levels, yielding a nonstandard CFP dataset located in another region of the multiparameter space. Comparison of the nonstandard CFPs of R. S. Puche *et al.*¹⁶ with the standard CFPs of Klimin *et al.*¹⁸ has led to a claim¹⁶ that the “formerly available (Ref. 18 here) adjusted phenomenological CFPs are expected to be somewhat dubious, especially as they are overly far from calculated semiempirical CFPs.” As discussed in

Sec. III, the claim¹⁶ critically assessing the CFPs (Ref. 18) turns out to be unjustified in view of the lack of standardization.^{1,2} The theoretical underpinning of the idea of standardization^{1,2} is provided by the transformation properties of the tensor operators used in the CF and ZFS Hamiltonians.¹⁹ The study of Ref. 19 has enabled derivation of the transformation expressions for the CFPs (ZFSPs) in the six basic regions of the multiparameter space for the CFP (ZFSP) components of rank $k=2, 4$, and 6 in orthorhombic¹ and monoclinic² symmetry. The inter-relationships between the CFPs (ZFSPs) expressed in different regions of the multiparameter space are crucial for meaningful interpretation and comparison of the experimental and/or theoretical results taken from various authors.^{2,14} Yet it appears from our comprehensive literature review that some authors are still unaware of the intrinsic properties of the orthorhombic and monoclinic symmetry CF (ZFS) Hamiltonians.

The major objective of this paper is to elucidate some subtle properties of orthorhombic¹ and monoclinic² Hamiltonians, especially those relevant for data interpretation and comparison, which appear not fully understood by some authors. We propose a framework for reanalysis of CFP datasets based on application of the standardization idea^{1,2} as well as the idea of dataset closeness. The closeness of any two CFP sets is represented by the closeness factor C_p and the norm ratio $R_p=N_A/N_B$ for the respective H_{CF} terms $k=2, 4, 6$, and the global ones C_{gl} . The peculiarities concerning orthorhombic and monoclinic symmetry CF (ZFS) Hamiltonians are briefly outlined in Sec. II. Three specific aims of this paper concern the illustrative examples taken from recent studies of the crystal-field splitting and magnetic behavior of $\text{Nd}_2\text{BaCuO}_5$ single crystals by R. S. Puche *et al.*¹⁶ and Klimin *et al.*¹⁸ These aims, dealt with in Sec. III, comprise (i) solution of the controversy¹⁶ arising from comparison of the nonstandard¹⁶ and standard¹⁸ CFPs as well as clarification of other inconsistencies concerning the results,¹⁶ (ii) determination of alternative physically equivalent CFP datasets, and (iii) application of the MCFT to improve the reliability of the final fitted results.^{2,14} Structural implications of the crystal-field analysis carried out in Section III and the inconsistencies in question are considered in Sec. IV.

The present study enables us to solve the problems in question and thus improve the understanding of the intricacies inherent in low-symmetry CFP datasets. Subsequently, a comparative analysis of the available CFPs for various trivalent rare earth R^{3+} ions, e.g., Nd, Er, and Eu in the series of crystals $R_2\text{BaXO}_5$ ($X=\text{Cu, Zn, Ni, and Co}$), as well as Eu dopant ions in Y_2BaZnO_5 and $\text{La}_2\text{BaZnO}_5$ crystals, will be carried out elsewhere.

II. PECULIARITIES OF ORTHORHOMBIC AND MONOCLINIC SYMMETRY CF HAMILTONIANS

A brief overview of the major notions and intrinsic features of CF Hamiltonians and the corresponding CFPs pertinent for orthorhombic and monoclinic symmetry is provided in this section. This is necessary for the present consideration and clarification of the problems in question. Within the $4f^N$ configuration, the general, i.e., triclinic, form of the CF

Hamiltonian^{9–12} can be written in terms of the many-electron spherical tensor operators (STOs) in the expanded form²⁰

$$H_{CF} = \sum_k B_{k0} C_{k0} + \sum_{k,q} \{ B_{kq} [C_{kq} + (-1)^q C_{k-q}] + i B_{k-q} [C_{kq} - (-1)^q C_{k-q}] \}, \quad (1)$$

where C_{kq} may represent, e.g., the Wybourne operators, which are nowadays most widely used in the CFT area,^{9–12} and B_{kq} are the real CF parameters which absorb the ligand factors, the $4f^N$ radial integrals, and the normalization factors of the unit tensors.^{9–12} The rank $k=2, 4$, and 6 terms are needed for the $4f^N$ ions at the centrosymmetric sites, whereas the components q in Eq. (1) adopt explicitly only positive values ($1 \leq q \leq k$). Equivalently, the extended Stevens (ES) operators^{19,21} and CFPs $B_k^q(\text{ES})$ are often used.^{12,20,22} Fitting the calculated energy levels obtained from diagonalization of the full Hamiltonian, including the free ion terms and H_{CF} in Eq. (1), to the observed spectra enables determination of the CFPs.^{9–12} Note that in Refs. 16 and 18 the form of H_{CF} is misprinted. The summation in H_{CF} of Ref. 16 should not run over $q=0$ since this may lead to confusion and potential double counting—this term needs to be listed explicitly as the first term in Eq. (1). In H_{CF} of Ref. 18 the operators are missing for the first three terms with $q=0$. In both cases, the incorrect form of H_{CF} will not affect the numerical results.

Intricate properties of H_{CF} and CFPs for the low-symmetry cases in question, which apply also to H_{ZFS} and ZFSPs, have been thoroughly considered in our earlier^{1,2,13} and more recent papers.^{14,15,23,24} In spite of their profound implications for the fitting process and data interpretation, these properties have been neither widely utilized in CF studies nor incorporated in the existing fitting and simulation computer programs as yet. Several intrinsic features of H_{CF} and CFPs that are of prime importance for the present considerations are briefly reviewed below.

(1) For the orthorhombic symmetry groups (C_{2v}, D_2, D_{2h}) there exist three mutually perpendicular and equivalent symmetry axes. The orthorhombic H_{CF} includes nine real B_{kq} in Eq. (1) with $q \geq 0$. The various choices of the axis system (x, y, z) with respect to the crystallographic axes result in different datasets $\{B_{kq}\}$. The six possible equivalent datasets of orthorhombic CF (ZFS) parameters are related by the standardization transformation $S_i(x', y', z')$, defined with respect to the original axis system $S_1(x, y, z)$, as follows: $S_2(x, -z, y)$, $S_3(y, x, -z)$, $S_4(y, z, x)$, $S_5(z, x, y)$, and $S_6(-z, y, x)$.¹

(2) For monoclinic symmetry groups (C_2, C_s, C_{2h}) there exists only one symmetry axis C_2 (or direction). Hence, besides the choice $z \parallel C_2$ in Eq. (1), two other choices are allowed,² i.e., $x \parallel C_2$ and $y \parallel C_2$ that correspond to the S_4 ($xyz \rightarrow yzx$) and S_5 ($xyz \rightarrow zxy$) transformations,¹ respectively. Standardization relations in the Stevens notation are listed in Table I of Ref. 2. Three approaches to fitting CFPs exist in the literature, denoted^{2,14,23} (*C*) *complete*—all 15 monoclinic CF parameters admissible by symmetry are taken into account; (*R*) *reduced*—one of the six “imaginary” CF parameters is set to zero by an appropriate rotation around the symmetry axis depending on the actual choice $x \parallel C_2$,

$y\|C_2$, or $z\|C_2$; and (A) *approximated*—only the “real” CF parameters are considered, resulting in an orthorhombic approximation of the actual monoclinic symmetry.

(3) In general, for orthorhombic and lower symmetry, the starting CFPs B_{kq} for fitting as well as the fitted ones may yield the “rhombicity” ratio $\kappa \equiv B_{22}/B_{20}$ anywhere between $-\infty$ and $+\infty$.^{1,2} The ratio κ may fall in any of the six different regions $(-\infty, -3/\sqrt{6})$, $(-3/\sqrt{6}, -1/\sqrt{6})$, $(-1/\sqrt{6}, 0)$, $(0, 1/\sqrt{6})$, $(1/\sqrt{6}, 3/\sqrt{6})$, and $(3/\sqrt{6}, +\infty)$. Hence, for any CFP dataset there exist five other datasets with varying κ values, all related by simple rotations and yielding identical energy level structure.^{1,2,14} This property of H_{CF} induces an arbitrariness in the choice of CFPs, which hinders their direct compatibility. This aspect has often been overlooked or ignored by the workers in the field.

(4) The existence of alternative physically equivalent yet numerically distinct CFP (ZFS) datasets for low symmetry implies that the fitted CFP (ZFS) datasets reported in the literature cannot be considered as unique. This creates a certain degree of arbitrariness, which may lead to confusion. To remedy this situation we have long proposed adopting a unique choice of the CFP datasets based on the simplest value of the ratio κ , i.e., confined to the range $(0, 1/\sqrt{6})$. This intrinsic property of orthorhombic and lower-symmetry H_{CF} (H_{ZFS}) allows confinement, by choosing a proper axis system,^{1,2} of the ratio κ in the Wybourne notation and $\lambda = B_2^2/B_0^2$ in the ES notation to the standard ranges $\{0, 0.4082\}$ and $\{0, 1\}$, respectively. This is the core of the standardization idea, which is applicable for both CFPs and ZFSPs. The idea, originally applied only for the orthorhombic rank $k=2$ ZFS terms, has been extended to the fourth- and sixth-order orthorhombic terms¹ as well as to monoclinic² and most recently triclinic symmetry.^{14,25} Note that alternative choices based on the method of reduction of three selected CFPs for triclinic symmetry have recently been proposed by Burdick and Reid.²⁶ Applications of the orthorhombic¹ and monoclinic² standardization to CFP datasets have been dealt with in Refs. 13–15, 23, and 24, and for the ZFS ones in Refs. 7 and 8. Using the superposition model, structural implications of standardization were also considered.⁷ It would be worthwhile if the standardization idea become more widely adopted in CF studies.

(5) Contrary to the implicit assumption by some authors,¹⁴ from the optical absorption spectra fittings it is not possible to determine the axis system in which the fitted CFPs are supposedly expressed. Our considerations¹⁴ pose an apparent dilemma: there is no prescription for assigning an axis system to the fitted CFPs. Hence, the notion of the *nominal* axis system has been introduced to solve this dilemma.¹⁴ In fact, as argued in Ref. 14 any fitted CFP dataset must initially be considered as expressed in an undefined nominal axis system denoted by (x_n, y_n, z_n) .

(6) As defined in Ref. 14, three types of CFP occur in the CF and optical studies, namely, (i) *symbolic CFPs*—defined by the symmetry-adopted CF Hamiltonians employed for a given ion-host system, and two types of numerical CFPs: (ii) *theoretical CFPs*—computed using model calculations, and (iii) *fitted CFPs*—obtained from fitting the experimental CF energy levels and/or intensity data to the theoretical predic-

tions based on the symmetry-adapted CF Hamiltonians. The general properties of the three types of CFP and the intrinsic properties specific for each type have been considered in Ref. 14.

For clarity, we provide also definition of the two basic quantities utilized in our considerations below. To assess the CF strength for CFP datasets for various transition ions in different compounds, the CF strength parameters S_k ($k=2, 4, 6$) defined as^{9,11}

$$S_k = \left[\left(\frac{1}{2k+1} \right) \left(B_{k0}^2 + 2 \sum_{q \neq 0} (B_{kq}^2 + B_{k-q}^2) \right) \right]^{1/2} \quad (2)$$

are used in the literature.^{2,14} The quantities S_k in Eq. (3) are the rotational invariants,^{2,14,23} since S_k remain the same for all CFP datasets transformed by any Euler angles (α, β, γ) , including each standardization transformation.^{1,2} In view of Noether’s theorem for the CF Hamiltonians invariant under continuous rotational symmetry,²³ the S_k ’s acquire a deeper meaning as specific second-order conserved quantities, yet not the only existing ones.

For quantitative comparison of CFPs (ZFSPs), the closeness factors C_k ($k=2, 4, 6$) and the global ones C_{gl} have been introduced.¹⁴ The closeness factors may be generalized to enable assessment of the closeness or divergence of any two same-nature datasets of N quantities, e.g., the CFPs or the energy levels, considered as N -dimensional “vectors” $\mathbf{A} = \{A_i\}$ and $\mathbf{B} = \{B_i\}$, $i=1-N$, in the corresponding N -dimensional parameter space. For the CFP datasets $\{B_{kq}\}$ of rank $k=2, 4$, and 6 , we have $N=(2k+1)$ and hence $i=1$ to $5, 8$, and 13 , respectively. Utilizing the normalized scalar product, the closeness factors for any two such vectors are defined as¹⁴

$$C = \frac{\sum_i A_i B_i}{\sqrt{\sum_i A_i^2} \sqrt{\sum_i B_i^2}} = \frac{\sum_i A_i B_i}{\sqrt{N_A} \sqrt{N_B}}. \quad (3)$$

Hence, $C \equiv C_k$ for the ZFSPs or CFPs of a given rank $k=2, 4$, and 6 or $C \equiv C_{gl}$ for the corresponding global factor for all k terms. In general, these factors will quantify the closeness, if approaching 1, or otherwise the divergence, if significantly different from 1.¹⁴ The quantities C_k and C_{gl} are especially useful for meaningful comparative analysis of low-symmetry CFPs (ZFSPs) taken from different sources.²⁵ In the course of the analysis of the orthorhombic and lower-symmetry²⁵ CFP datasets, we have realized that in these cases the definition of the closeness factors¹⁴ in Eq. (3) must be modified. It turns out that the values of the closeness factors in the range $(0, 1)$, implied by Eq. (3), are valid only for fully compatible datasets, i.e., those belonging to the same region of the parameter space, so not necessarily the standard region.¹⁴ Additionally, in order to describe the closeness of any two vectors more comprehensively, we have recently additionally considered²⁷ the ratio of the norms N_A and N_B defined in Eq. (3): $R = N_A/N_B$ [in percent or rescaled to the range $(0, 1)$ for $N_A \leq N_B$ or $(1, \infty)$ for $N_A \geq N_B$]. The explicit expressions for the closeness factors C and the norms ratios R applicable for major operator notations as

TABLE I. The theoretical crystal field parameters B_{kq} in the Wybourne notation calculated by R. S. Puche *et al.* (Ref. 16) using the semiempirical simple overlap model for Nd^{3+} ion in $\text{Nd}_2\text{BaCuO}_5$ single crystals together with the alternative physically equivalent CFP datasets (Si) obtained using the package CST; bold sets indicate the standardized CFPs.

Set	B_{20}	B_{22}	κ	B_{40}	B_{42}	B_{44}	B_{60}	B_{62}	B_{64}	B_{66}
S1	-645	-437	0.678	-1055	-1386	280	107	775	416	-228
S2	857.7	176.5	0.206	-1198.5	-1295.2	400.1	-605.0	-675.7	225.7	375.3
S3	-645	437	-0.678	-1055	-1386	280	107	-775	416	228
S4	-212.7	613.5	-2.884	992.9	90.77	-1433.4	-45.5	464.8	375.2	-688.1
S5	857.7	-176.5	-0.206	-1198.5	1295.2	400.1	-605.0	675.7	225.7	-375.3
S6	-212.7	-613.5	2.884	992.9	-90.77	-1433.4	-45.53	-464.8	375.2	688.1
S_k	$S_2=399.5$			$S_4=753.6$			$S_6=357.6$			

well as their general properties have been discussed in Ref. 27. Note that, unlike the CFP datasets, the energy level sets form fully compatible datasets. Since R. S. Puche *et al.*¹⁶ have used the energy levels reported by Klimin *et al.*¹⁸ there is no point in carrying out the closeness factor analysis for their energy level datasets. Application of the generalized closeness definitions²⁷ to the energy level sets obtained by various authors for Pr^{4+} ions doped in BaPrO_3 has been considered in Ref. 25.

III. CRYSTAL-FIELD ANALYSIS OF Nd^{3+} IONS IN $\text{Nd}_2\text{BaCuO}_5$ AND $\text{Nd}_2\text{BaZnO}_5$

As illustrative examples for comparative CF analysis based on application of the standardization and closeness factors we consider in this section the CFPs for Nd^{3+} ions in $\text{Nd}_2\text{BaCuO}_5$ and $\text{Nd}_2\text{BaZnO}_5$. Calculations are facilitated by two computer packages. (1) The computer package^{28,29} CST has been developed to handle various manipulations of CFPs and ZFSPs: (i) *conversions* between various unit as well as several tensor operator notations, including the ESO (Refs. 19–21) and STO (Refs. 20 and 22) notations, (ii) *standardization*,^{1,2} and (iii) *transformations*.¹⁹ It also incorporates (iv) rotational invariants^{2,14,23} S_k and (v) the error

analysis for the transformed B_{kq} (B_k^q) parameters. The package^{28,29} CST provides useful tools for comparison of apparently different but physically equivalent nonstandard CFP (Refs. 13–15, 24, and 25) and ZFSP (Refs. 7 and 8) datasets expressed in various notations and axis systems as well as for generation of the correlated equivalent sets. (2) The most recently developed computer package²⁵ DPC comprises three modules: (i) procedure for *3 dimensional* diagonalization (3DD) of the second-rank CFPs, (ii) extension of the *pseudosymmetry-axis* method to lower-symmetry cases that enables finding the pseudosymmetry-axis system for the fourth-rank CFPs, and (iii) calculation of the *closeness* factors and the norm ratios for quantitative comparison of CFP datasets and other quantities. Both computer packages may be obtained from the authors on a collaborative basis. Regarding other aspects pertinent for any analysis of the CFPs and ZFSPs, it may also be useful to consult Refs. 30 and 22 on the spin Hamiltonian formalisms, the review of the often confused interrelations between the CF and ZFS quantities,³¹ and the note on the incorrect orthorhombic ZFSPs relations.³²

The original and transformed CFPs are presented in the tables: the semiempirical CFPs calculated using the simple overlap model (SOM) (Table I) and fitted CFPs (Table II), of R. S. Puche *et al.*¹⁶ for the Nd^{3+} ion in $\text{Nd}_2\text{BaCuO}_5$, the fitted

TABLE II. The CFPs B_{kq} fitted by R. S. Puche *et al.* (Ref. 16) using the experimental energy levels of Klimin *et al.* (Ref. 18) and taking their SOM-calculated CFPs as the initial CFPs for Nd^{3+} ion in $\text{Nd}_2\text{BaCuO}_5$. Bold sets indicate the standardized CFPs.

Set	B_{20}	B_{22}	κ	B_{40}	B_{42}	B_{44}	B_{60}	B_{62}	B_{64}	B_{66}
S1	-480	213	-0.444	-1336	-1641	35±49	720±	104	270	-346
	±21	±13		±44	±24		43	±38	±35	±48
S2	-20.9	400.4	-19.16	-1761.7	-1371.8	391.2	-152.4	-572.6	36.9	-349.0
S3	-480	-213	0.444	-1336	1641	35	720	-104	270	346
S4	500.9	187.4	0.374	832.9	269.3	-1779.7	-676.5	19.0	-103.2	-472.0
	±19.1	±14.4		±57.1	±38.7	±28.6	±58.8	±41.8	±35.0	±34.6
S5	-20.9	-400.4	19.16	-1761.7	1371.8	391.2	-152.4	572.6	36.85	349.0
S6	500.9	-187.4	-0.374	832.9	-269.3	-1779.7	-676.5	-19.04	-103.2	472.0
S_k	$S_2=253.4$			$S_4=892.8$			$S_6=266.8$			

TABLE III. The CFPs B_{kq} fitted by Klimin *et al.* (Ref. 18) from the experimental absorption spectra for Nd^{3+} ion in $\text{Nd}_2\text{BaCuO}_5$ single crystals. Bold sets indicate the standardized CFPs.

Set	B_{20}	B_{22}	κ	B_{40}	B_{42}	B_{44}	B_{60}	B_{62}	B_{64}	B_{66}
S1	481	44	0.091	843	534	1734	966	180	201	-7
S2	-294.4	-272.6	0.926	2551.7	-546.7	304.4	-551.5	-444.2	-204.6	-384.9
S3	481	-44	-0.091	843	-534	1734	966	-180	201	7
S4	-186.6	-316.6	1.697	1707.4	-1080.7	1010.8	-334.3	-243.2	-146.5	-634.8
S5	-294.4	272.6	-0.926	2551.7	546.7	304.4	-551.5	444.2	-204.6	384.9
S6	-186.6	316.6	-1.697	1707.4	1080.7	1010.8	-334.3	243.2	-146.5	634.8
S_k	$S_2=216.9$			$S_4=900.3$			$S_6=288.1$			

CFPs of Klimin *et al.*¹⁸ for the Nd^{3+} ion in $\text{Nd}_2\text{Ba}(\text{Zn}, \text{Cu})\text{O}_5$ (Table III), and the experimental CFPs of Taibi *et al.*³³ for the Nd^{3+} ion in $\text{Nd}_2\text{BaZnO}_5$ (Table IV) that were used as the initial ones for fittings in Ref. 18. Note that Klimin *et al.*¹⁸ consider the CFPs for the Nd^{3+} ion in $\text{Nd}_2\text{BaCuO}_5$ as identical with those for the Nd^{3+} ion in $\text{Nd}_2\text{BaZnO}_5$. The transformed CFPs are obtained from the original CFPs employing the orthorhombic standardization transformations S_i (defined in Sec. II) incorporated into the package CST.^{28,29} The transformed CFPs include the standardized CFPs, whenever appropriate, and their respective errors, if available. All sets in each Table I–IV represent numerically distinct yet implicitly physically equivalent CFP datasets. Each correlated set belongs to a different region of the multiparameter space and yields the same energy levels. These sets or, even better, slightly modified ones, may be used as the initial sets for several additional independent fittings. This is the cornerstone of the multiple correlated fitting technique,^{2,14} which has been applied for the first time to several R -ion–host systems.¹³

It is of interest to utilize the available experimental data¹⁸ to perform several refittings using the transformed datasets provided in Tables I–IV. The procedure used was as follows. Concerning the free-ion parameters, E_{av} , F^k , α , β , ζ , T^3 , T^4 , T^6 , T^7 , M^0 , and P^2 were allowed to vary freely during the fittings. Their starting values were taken as the fitted ones in the respective sources.^{16,18} R. S. Puche *et al.*¹⁶ used the matrix element $\langle {}^2H_{2,1/2} | U^4 | {}^2H_{2,1/2} \rangle$ reduced by 4, whereas Klimin *et al.*¹⁸ omitted in their calculations the energy levels

${}^2H_{2,1/2}$. Since in the Reid *et al.* program¹³ used by us for fittings the reduction of the matrix element is feasible only with respect to the whole 2H_2 term, i.e., $\langle {}^2H_2 | U^4 | {}^2H_2 \rangle$, but not for each J component separately, to enable comparison we carry out fittings for two sets of experimental energy levels, namely, (A) with and (B) without the energy levels ${}^2H_{2,1/2}$. Our current experience with the MCFT calculations indicates that the correlated initial CFPs after modification by up to 50% return the fitted CFPs still within the same region of the multiparameter space. In the present MCFT calculations, for each set in Tables II and III we have generated two additional sets varying by + and -5% the CFPs in a given set. All fittings were carried out using these three sets as the starting sets, yielding 18 fitted sets of types A and B. Since the space limitations prevent us from providing all outputs in a tabular form, we rather summarize our overall results, and provide the averaged CFPs resulting from the MCFT calculations in Table V.

Using (i) the fitted (set S1 in Table III, denoted by IIISI) and (ii) the initial (set IVS1) CFPs of Klimin *et al.*¹⁸ as the initial CFPs for our fittings, we obtain two pairs of nearly identical sets (iA and iiA) and (iB and iiB) representing the same minimum; both sets differ slightly from the original set IIISI. The insignificant differences may be due to the use of different computer programs (Reid *et al.*'s program¹³ by us and Porcher¹⁷ in Ref. 16). The latter program has, most probably, also been used by Klimin *et al.*¹⁸ Comparison of the sets iA and iB and iiA and iiB shows that taking into account the energy levels ${}^2H_{2,1/2}$ yields somewhat different rms val-

TABLE IV. The CFPs B_{kq} fitted by Taibi *et al.* (Ref. 33) from the experimental absorption spectra for Nd^{3+} ion in $\text{Nd}_2\text{BaZnO}_5$ single crystals. Bold sets indicate the standardized CFPs.

Set	B_{20}	B_{22}	κ	B_{40}	B_{42}	B_{44}	B_{60}	B_{62}	B_{64}	B_{66}
S1	786.0	73.3	0.093	873.6	102.0	1523.0	1055.2	497.1	-104.6	-173.5
	±20	±29		±46	±64	±19	±43	±54	±44	±42
S2	-482.8	-444.7	0.921	2001.0	-611.1	579.7	-409.9	-704.7	-496.2	-134.4
S3	786.0	-73.3	-0.093	873.6	-102.0	1523.0	1055.2	-497.1	-104.6	173.5
S4	-303.2	-518.0	1.708	1839.8	-713.1	714.7	-102.8	64.7	-414.1	-814.8
S5	-482.8	444.7	-0.921	2001.0	611.1	579.7	-409.9	704.7	-496.2	134.4
S6	-303.2	518.0	-1.708	1839.8	713.1	714.7	-102.8	-64.7	-414.1	814.8
S_k	$S_2=354.6$			$S_4=776.2$			$S_6=360.5$			

TABLE V. The CFPs B_{kq} resulting from the present MCFT calculations averaged over 18 independently fitted sets and two types for the two major starting CFP sets from Ref. 18 (i) and Ref. 16 (iii) for Nd^{3+} ion in $\text{Nd}_2\text{BaZnO}_5$ single crystals; Δ_p denotes the mean difference (see text).

p	{iA}	Δ_{iA}	{iB}	Δ_{iB}	{iAB}	Δ_{iAB}	{iiiA}	Δ_{iiiA}	{iiiB}	Δ_{iiiB}	{iiiAB}	Δ_{iiiAB}
B_{20}	502.0	0.0	502.3	0.0	502.1	0.1	515.4	0.1	518.8	0.0	517.1	1.7
B_{22}	27.9	0.1	39.9	0.0	33.9	6.0	22.7	0.0	21.8	0.1	22.2	0.4
κ	0.056		0.079		0.068		0.044		0.042		0.043	
B_{40}	847.7	0.2	841.5	0.0	844.7	3.2	640.4	0.4	632.2	0.2	636.3	4.1
B_{42}	548.3	0.1	520.8	0.0	534.6	13.7	-475.6	0.4	-464.7	0.0	-470.1	5.5
B_{44}	1701.1	0.0	1725.7	0.0	1713.4	12.3	-1756.5	0.1	-1744.1	0.1	-1750.3	6.2
B_{60}	989.3	0.1	952.6	0.0	971.0	18.4	-860.7	0.2	-912.6	0.7	-886.6	25.9
B_{62}	148.9	0.4	156.0	0.0	152.4	3.5	105.3	0.6	109.1	1.4	107.2	1.9
B_{64}	205.8	0.1	209.9	0.0	207.9	2.0	-273.8	0.1	-286.1	0.7	-279.9	6.1
B_{66}	-7.7	0.4	-0.5	0.0	-4.1	3.6	261.1	0.4	255.0	1.0	258.1	3.0
S_2	225.2		226.0		225.6		230.9		232.4		231.7	
S_4	888.7		894.8		891.7		884.0		876.5		880.3	
S_6	291.9		283.4		287.7		284.1		297.5		290.8	

ues; however, it does not affect significantly the values of the fitted CFPs. On the other hand, using the fitted (set IIS1) CFPs of R. S. Puche *et al.*¹⁶ as the initial CFPs for our fittings yields a completely different minimum (sets iiiA and iiiB) from the set IIS1. Moreover, the value of the rms (24.7 and 26.5 cm^{-1} , respectively) is much larger than that given by the authors of Ref. 16. The difference in the rms values between the energy levels generated based on the adjustable free-ion parameters together with the CFPs (IIS1) (Ref. 16) and the experimental levels¹⁸ is 28.2 cm^{-1} , whereas the largest difference of -119.7 cm^{-1} appears between the calculated energy level and the observed one at 28 514 cm^{-1} . Additionally, we note that freeing the parameters M^0 and P^2 during fitting using the starting CFP IIS1 set¹⁶ results in too small values of these parameters ($M^0 \sim 1.17-1.22 \text{ cm}^{-1}$ and $P^2 \sim 110-130 \text{ cm}^{-1}$). No such problems are encountered using the starting CFP IIS1 set;¹⁸ these fittings yield reasonable values of the parameters M^0 and P^2 . Finally, using the SOM (set IS1) CFPs (Ref. 16) as the initial CFPs for our fittings yields the fitted CFPs different than those obtained by the authors.¹⁶ Importantly, the CFPs fitted by us yield substantially smaller rms values, thus indicating a better minimum. Hence, it seems that the fitted¹⁶ CFPs correspond most probably to a local minimum and not a global one. One reason for the difference in question may be due to the fourfold reduction of the matrix element $\langle {}^2H_{211/2} | U^4 | {}^2H_{211/2} \rangle$ by R. S. Puche *et al.*¹⁶ However, our fittings do not indicate any significant effect of including or neglecting the energy levels ${}^2H_{211/2}$ in the calculations. Moreover, if such modification of this quantity significantly affects other energy levels and the resulting minimum, the reliability of the fitted results¹⁶ will be further diminished. Note that for the starting CFPs,¹⁶ the least-squares procedure converges more slowly in about 14 iterations as compared with five iterations in the case of the starting CFPs.¹⁸

The basic idea of the MCFT approach is that instead of the one-line fittings adopted in Refs. 16 and 18 we perform a

number of independent yet correlated fittings of the experimental energy levels starting from distinct regions in the parameter space. In the present case, using the CFPs of each set S_i in Tables II and III and the two additional $\pm 5\%$ sets as the starting sets, a total of 18 fittings of each type A and B were performed for the original energy levels.¹⁸ In general, this procedure yields one standard CFP set and five nonstandard CFP sets independently fitted. The latter sets are then transformed using the package^{28,29} CST into the standard region for overall comparison and intercorrelation. We note that our fittings using the starting CFPs of Ref. 16 yield worse minima (rms 24.7 cm^{-1}) than for the starting CFPs of Ref. 18 (rms 14.6 cm^{-1}). Hence, it is likely that the minimum obtained in either of the two cases is rather a local one (probably that obtained using the CFPs of R. S. Puche *et al.*¹⁶). Nevertheless, starting from distinct S_i regions (for each given set as well as for the corresponding sets varied by + and -5%) yields the same solution. This indicates that a given local minimum transforms into various S_i regions in the multiparameter space. It turns out that the absolute difference between the smallest and the largest values of any CFP fitted in these correlated ways and then transformed to the standard range, is below 10 cm^{-1} , whereas on average this variance is below 3 cm^{-1} . This variance is much smaller than the uncertainty in the CFP determination, which reaches several tens of cm^{-1} . The values of CFP obtained in any given S_i region for each given set and the two additional $\pm 5\%$ sets differ mostly at the order of a fraction of cm^{-1} to a maximum of a few cm^{-1} .

The independently fitted and standardized CFPs resulting from the present MCFT calculations for each of the two major starting CFP sets^{16,18} and the two types A and B, i.e., the sets $p=\{iA\}$, $\{iB\}$, and $\{iAB\}$ and $p=\{iiiA\}$, $\{iiiB\}$, and $\{iiiAB\}$, were averaged over 18 fitted sets and two types. In view of the similarity of the MCFT-obtained sets (iA and iiA) and (iB and iiB), the averaged values are listed in Table V only for the sets $\{iA\}$ and $\{iB\}$. The averaged CFP values together with the mean difference $\Delta_p \equiv (1/n) \sum_n |B_{kq}^{(av)} - B_{kq}^{(n)}|$

TABLE VI. The closeness factors C_p (dimensionless) and the norm ratios R_p (%) for the pairs (XS_i, YS_j) of the respective standard CFP datasets listed in the indicated Tables X and Y ($X, Y=I, II, III, \text{ and } IV$).

p type	Pair					
	(IS2, IIS4)		(IS2, IIIS1)		(IS2, IVS1)	
	C_p	R_p	C_p	R_p	C_p	R_p
2	0.979375	157.6	0.988081	184.2	0.988460	78.77
4	-0.515232	84.41	-0.164758	83.71	-0.017574	94.26
6	-0.013917	134.1	-0.554152	124.2	-0.887500	98.41
Global	-0.330805	94.8	-0.163513	93.79	-0.114953	97.81

p type	Pair					
	(IIIS1, IVS1)		(IIS4, IIIS1)		(IIS4, IVS1)	
	C_p	R_p	C_p	R_p	C_p	R_p
2	0.999997	61.18	0.936600	116.8	0.937465	71.48
4	0.974181	115.98	-0.716404	99.17	-0.743676	115.0
6	0.858149	79.90	-0.682150	92.61	-0.407542	74.00
Global	0.939594	105.45	-0.658514	98.90	-0.585475	104.3

are listed in Table V. Keeping in mind that the ${}^2H_{2,11/2}$ levels were observed experimentally, they should have been included in the fittings in spite of the fact that the CF model does not account well for their energies. Our calculations indicate that including the ${}^2H_{2,11/2}$ levels or neglecting them do not influence the fitted CFPs to any appreciable degree. Thus we conclude that the sets {iB} and {iiiB} in Table V may be considered as in most reliable final sets.

Three major advantages of the applications of the MCFT are as follows. First, the independently fitted CFP sets transformed into the standard region enable improving the reliability of the final fitted results since, by averaging over the total number of intercorrelated sets, the uncertainty in the determination of the final CFPs is reduced. Second, a good correlation of the final fitted CFP sets ensures that for a given starting CFP sets we have reached the same minimum; so we cannot distinguish with certainty whether a given solution corresponds to a local or global minimum, the spurious minima may be excluded in this way. Thus the MCFT results confirm the conclusions which may be obtained considering the convergence of the least-squares fitting procedure. Third, the MCFT illustrates convincingly the physical equivalence of the several correlated CFP sets belonging to different regions of the multiparameter space. These advantages have not been appreciated by most researchers as yet. Wider application of the MCFT utilizing the starting CFPs obtained in the distinct regions in the parameter space, instead of the one-line fittings commonly adopted in the literature, is recommended in future CF studies. From the point of view of the fitting procedure and putting aside the question of the “truthfulness” of the fitted CFPs, which depends on the starting CFP values, we conclude that the CFPs reported by Klimin *et al.*¹⁸ may be reckoned as more credible than those of R. S. Puche *et al.*¹⁶ This is contrary to the claim by the latter authors labeling the former authors’ CFPs as dubious.

Comparative analysis of the CFP datasets listed in Tables I–IV is facilitated by the closeness factors C_p and the norm ratios R_p ($p=2, 4, 6, \text{ and } \text{gl}$) for the CFP dataset pairs $(XS_i,$

$YS_j; X, Y=I, II, III, \text{ and } IV)$. The quantities C_p measure the relative departure of the angle between the given two vectors from zero, i.e., for the same orientation $C_p=1$, whereas R_p measure the relative difference in the vectors lengths, i.e., for the same length $R_p=1$ (or 100%). To illustrate the problems with incompatible datasets mentioned in Sec. II, we calculated C_p and R_p for the two original S1 sets¹⁶ in Tables I and II. Only C_4 is close to 1 (0.9872), while C_2 (0.2438) and C_6 (0.5004) differ significantly from 1, whereas $R_p=158\%$, 84% , and 134% for $p=2, 4, \text{ and } 6$, respectively. This may apparently indicate smaller disparity between these two sets than for their standardized counterparts, i.e., the pair (IS2, IIS4) in Table VI. However, a deeper analysis of the general properties of C_p and R_p carried out in Ref. 27 reveals that special considerations are necessary for a meaningful interpretation of the values of C_p and R_p for orthorhombic CFP (ZFSP) datasets belonging to two different regions of the parameter space.¹⁴ In the present case, the sets S1 in Tables I and II are both nonstandard and can be standardized by transformations S2 and S4, respectively. This means that the original S1 sets¹⁶ belong to two different regions of the parameter space¹⁴ and thus cannot be directly compared, contrary to the implicit assumption used in Ref. 16. Hence, the values of C_p and R_p given above for the pair (IS1, IIS1) are not meaningful.

It turns out²⁷ that for such incompatible sets the range of the values of C_p (0, 1), implied by Eq. (3), is not valid, and, moreover, irrespective of the operator notation used for H_{CF} , the quantities C_p are not invariant under rotations of the axis system. On the other hand, the invariance of the R_p values under rotations of the axis system depends on the operator notation used for H_{CF} . Other points arising from these considerations²⁷ and relevant for the present discussion are summarized below. For any two orthorhombic CFP (ZFSP) datasets belonging to two different regions of the parameter space, the lengths of the vectors vary with the regions depending on the notation used. Since the ES operators are not normalized, the length of a vector $\{B_{\chi}^q(\text{ES})\}$, i.e., its norm

defined as $N_k \equiv \sum_{-k \leq q \leq +k} [B_k^q]^2$, changes after any transformation, including the standardization transformations Si .^{1,2} Hence, the rotational invariants S_k , which play a similar role to the norms, have been defined²³ based on the normalized Stevens (NS) operators.^{19,20} Moreover, it turns out that the NS notation provides a more accurate representation of the relative values of the CFPs, whereas the ES notation yields apparently misleading ratios of the CFPs due to different normalization factors for the q components.²⁵ For the Wybourne CFPs, care must be taken to include, in the calculation of the quantities C_p and R_p , all CFPs involved in a given CF Hamiltonian form, i.e., either the compact or expanded form.^{20,34} The compact form by itself represents explicitly all CFPs and hence Eq. (3) yields proper results. However, the expanded form with one CFP associated with a combination of two operators as in Eq. (1) requires modification of Eq. (3).²⁷

Using the proper definitions,²⁷ for a meaningful comparison of the CFP datasets^{16,18,33} we have calculated in Table VI the quantities C_p and R_p for all pairs (Si, Sj) of CFPs expressed in the standard range as listed in Tables I–IV. The values of C_p and R_p for the experimental³³ CFPs used as the initial ones in Ref. 18 (set S1 in Table IV and the fitted¹⁸ CFPs (set S1 in Table III) indicate near-perfect closeness of the two CFP datasets. On the other hand, no such good correlation is observed for the initial SOM set S2 in Table I and the fitted set S4 in Table II of R. S. Puche *et al.*,¹⁶ which after standardization by us belong to the same standard region of the parameter space,¹⁴ and thus are directly comparable. There is a partial closeness concerning the angles and/or lengths for some quantities $p=2, 4, 6$, and gl, but overall a disparity between the two sets is observed. In general, this finding is not surprising as the fitted sets may be quite far off the initial ones. More important for the present considerations is the closeness, or otherwise, between the standardized sets¹⁶ in Table I (S2) or Table II (S4) and the S1 set¹⁸ in Table III criticized in Ref. 16. The values of C_p and R_p in Table VI for the pairs (IS2, IIS1) and (IIS4, IIS1) indicate considerable closeness concerning the angles and/or lengths for most of the quantities $p=2, 4, 6$, and gl. Overall moderate but not perfect closeness between these sets^{16,18} is observed, apart from the opposite signs of some CFPs, which result in negative C_p values. Possible reasons for the differences in signs require consideration of the axis systems carried out in Sec. IV.

The closeness analysis for the averaged CFP sets listed in Table V is carried out in Table VII. The closeness factors C_p and the norm ratios R_p ($p=2, 4, 6$, and gl) for the two types of CFP set A and B indicate that the energy levels ${}^2H_{21/2}$ makes virtually no difference concerning the fittings of the experimental energy levels, regardless of the starting CFPs used, i.e., either from Ref. 18 or 16. The final averaged CFP sets, i.e., {iAB} and {iiiAB}, turn out to be not so close in terms of C_p , whereas the values of R_p indicate significant closeness. Cross comparison of the results in Table VI IIS4, IIS1) and VII ({iAB}, {iiiAB}) reveals greater closeness of the final averaged CFP sets obtained from the two starting CFP sets used than in the case of the original standardized sets. The question of sign ambiguity reflected in the negative signs of the closeness factors C_p for the pair ({iAB}, {iiiAB}) is discussed in Sec. IV.

TABLE VII. The closeness factors C_p (dimensionless) and the norm ratios R_p (%) for the pairs of the averaged CFP datasets resulting from the MCFT calculations listed in Table V.

p type	Pair					
	({iB}, {iAB})		({iiiB}, {iiiAB})		({iAB}, {iiiAB})	
	C_p	R_p	C_p	R_p	C_p	R_p
2	0.9999	100.43	1.0000	99.36	0.9994	94.79
4	1.0000	100.70	1.0000	100.85	-0.8441	102.62
6	0.9999	97.07	0.9999	95.48	-0.8707	97.89
Global	0.9999	100.23	0.9999	100.09	-0.7902	101.74

p type	Pair					
	({iA}, {iAB})		({iiiA}, {iiiAB})		({iAB}, {iiiAB})	
	C_p	R_p	C_p	R_p	$ C_p $	R_p
2	0.9999	99.67	1.0000	100.64	0.9994	94.79
4	1.0000	99.31	1.0000	99.16	0.9962	102.62
6	0.9999	102.99	0.9999	104.68	0.9308	97.89
Global	0.9999	99.79	0.9999	99.93	0.9878	101.74

The major outcomes of the standardization, MCFT, and closeness analysis carried out in this section are (i) the original CFPs for the Nd^{3+} ion in $Nd_2Ba(Cu,Zn)O_5$ from both sources^{16,18} are not comparable and thus no meaningful conclusion can be obtained from their direct comparison, (ii) only after proper standardization does the fitted¹⁶ CFP dataset become directly comparable with the standard¹⁸ one, (iii) by averaging over the total number of intercorrelated sets obtained from the MCFT, the reliability of the determination of the final CFPs increases substantially, (iv) the two sets^{16,18} appear more compatible with each other than the direct, albeit meaningless, comparison of the original two sets done by R. S. Puche *et al.*¹⁶ would show, and (v) the observed moderate closeness of the CFP datasets^{16,18} after proper standardization is confirmed by comparison of the values of the rotational invariants S_k listed in Tables I–IV. Thus, in view of these outcomes, the claim of R. S. Puche *et al.*¹⁶ ascribing dubious nature to the CFPs of Ref. 18 based on their apparent disparity as being “overly far from calculated semiempirical CFPs” turns out to be unjustified. Hence, the present considerations enable us to solve the controversy in question and thus improve the understanding of the intricacies inherent in low-symmetry CFP datasets. The reasons for any remaining disparity indicated by the observed moderate and not perfect closeness between the standardized CFPs of Refs. 16 and 18 must be searched for in a different realm. The possible reasons for such disparity may be related either to (i) the factors related to the SOM and intrinsic approximations made in this semiempirical procedure or (ii) the fitting procedures used by the authors.¹⁶ Note that various theoretical models,³⁵ e.g., the superposition model, angular overlap model, and exchange charge model, to name a few, may yield varying results even if the same crystallographic data serve as input. Various other reasons are considered in Sec. IV.

IV. STRUCTURAL IMPLICATIONS OF THE CRYSTAL-FIELD ANALYSIS

An aspect important for comparative analysis of any two CFP datasets concerns the actual axis system (AS) in which they are expressed. However, as discussed in Ref. 14, any original fitted set, e.g., the sets S1 in Table II–IV, can be assigned only to an unspecified nominal axis system. On the other hand, any original model set, e.g., the set S1 in Table I, must have been theoretically calculated in a well-specified axis system. It appears that the AS used to calculate the SOM parameters¹⁶ may differ from the actual symmetry-adapted AS (SAAS) for Nd³⁺ ions in Nd₂BaCuO₅. Note that the theoretical calculations of CFPs based on various models, which most commonly employ the crystallographic AS (CAS) centered at the R ion, may yield tricliniclike CFP datasets. However, “triclinicity” of the model CFPs turns out to be apparent in the cases when (i) the local site symmetry (LSS) is actually higher than triclinic or (ii) the crystallographic AS does not coincide with the symmetry-adapted AS.²⁵ Inspection of the crystallographic data¹⁶ and the structure of the local environment of Nd³⁺ ions in Nd₂BaCuO₅ (see Fig. 1 in Refs. 16 and 18) reveals that indeed the CAS does not coincide with the SAAS. To verify the local structural relationships, we have used the crystallographic data¹⁶ to generate the three-dimensional graph of (i) the Nd-O₈ complex [Fig. 1(a)] and (ii) the unit cells in Nd₂BaCuO₅ [Fig. 1(b)]. Our Fig. 1, which is compatible with Fig. 1 in Ref. 18, confirms the noncoincidence of the CAS with the SAAS as well as the assignment of the LSS as C_{2v} . For the complex in Fig. 1(a), the C_2 symmetry axis is oriented along the intersection of the two σ_v planes, i.e., it lies in the ab plane at an angle of about 135° toward the a axis. Moreover, the unit cell graph [Fig. 1(b)] reveals the existence of four crystallographically equivalent but magnetically inequivalent Nd³⁺ sites in the unit cell. Each such site has differently oriented symmetry axes; neither of these axes coincides with the CAS.

The above structural relationships have important implications for the comparative analysis in question. It appears that R. S. Puche *et al.*¹⁶ might have omitted the nonorthorhombic CFPs from the SOM calculations. Had they included the lower-symmetry CFPs, the nonzero triclinic CFPs would also have been obtained in the CAS. Transformation of such CFPs from the CAS to an appropriate SAAS should bring all nonorthorhombic CFPs to zero. On the other hand, had they carried out the SOM calculations in the SAAS suitable for the actual orthorhombic LSS, different set of only orthorhombic CFPs would have been obtained, with all triclinic CFPs being zero. Importantly, neither the definition of the axis system used to calculate the SOM parameters¹⁶ was provided, nor was the distinction between the CAS and SAAS discussed by the authors. Hence, we are not in the position to clarify in which axis system the SOM CFPs were actually calculated by R. S. Puche *et al.*¹⁶ It is highly probable that the subtle points discussed above have escaped the authors’ attention. This may be one of the reasons for the overall disparity between the standardized sets, i.e., the SOM-calculated CFP dataset (S2 in Table I) and the fitted one¹⁶ (S4 in Table II) discussed in Sec. III.

It is worthwhile to compare directly the fitted standardized CFPs (S4 in Table II) of R. S. Puche *et al.*,¹⁶ taking into

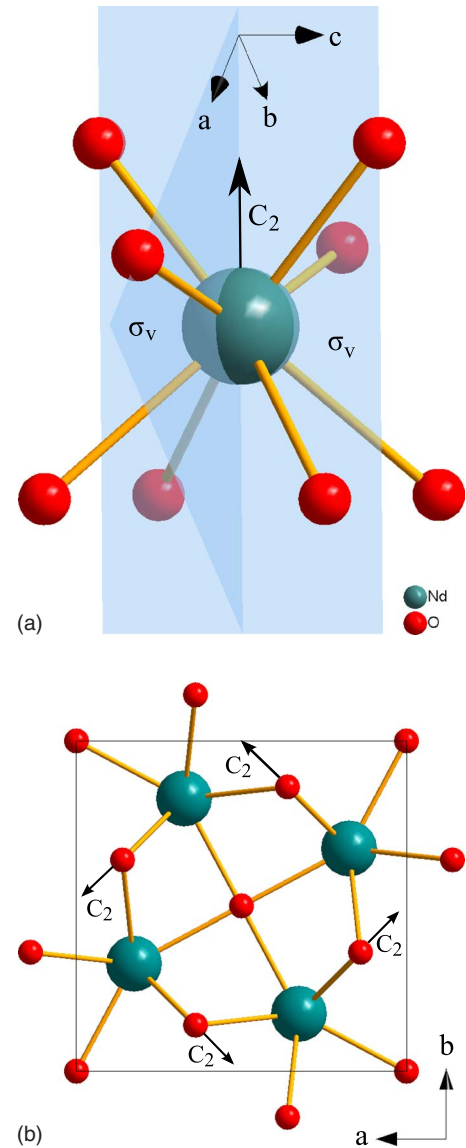


FIG. 1. (Color online) Structure of Nd₂BaCuO₅: (a) one of the four Nd-O₈ complexes with the CAS indicated, and (b) four crystallographically equivalent Nd-O₈ complexes in the unit cell projected on the ab plane.

account their corresponding uncertainties, and the CFPs of Klimin *et al.*¹⁸ We notice that the absolute values of the most significant CFPs namely, B_{20} , B_{40} , and B_{44} , are very close. The sign difference in B_{44} for the two sets may be due to the ambiguity in the sign determination, observed, e.g., by Burdick *et al.*^{36,37} In fact, a rotation 45° about O_z changes the sign of B_{44} and B_{64} , while leaving B_{k0} invariant, whereas other CFPs transform into their “ $-q$ ” counterparts having the same value without the sign change: $B_{22} \rightarrow B_{2-2}$, $B_{42} \rightarrow B_{4-2}$, $B_{62} \rightarrow B_{6-2}$, $B_{66} \rightarrow B_{6-6}$. Fittings done by R. S. Puche *et al.*¹⁶ using a fixed orthorhombic H_{CF} form for C_{2v} symmetry could be repeated using a triclinic H_{CF} form. Since the latter form does not impose restrictions on the symbolic¹⁴ CFPs, both the original case and that rotated by 45° about O_z could be handled. In each of the two cases, one could obtain

different, yet correlated, sets of CFPs, each with some specific CFPs being zero.

In view of the feasible sign ambiguity in the fitted CFPs,^{16,18} we consider also the “absolute” equivalents of the closeness factors $|C|$ calculated disregarding the signs of CFPs:

$$|C| = \frac{\sum_i |A_i||B_i|}{\sqrt{\sum_i A_i^2} \sqrt{\sum_i B_i^2}} = \frac{\sum_i |A_i||B_i|}{\sqrt{N_A} \sqrt{N_B}}. \quad (4)$$

For the pair (IIS2, IIS1), i.e., with both sets in the standard range, we obtain $|C_2|=0.9366$ and $|C_4|=0.9901$, i.e., very close to 1, while $|C_6|=0.7091$ differs from 1; all R_p are close to 100%, being 117%, 99%, and 93% for $k=2, 4$, and 6 , respectively. This indicates considerable closeness of the magnitudes of CFPs in these two datasets, contrary to the criticism¹⁶ based, inappropriately, on comparison of the directly incomparable datasets.^{16,18} The absolute equivalents of the closeness factors $|C_p|$ for the MCFT-obtained CFPs ($\{iAB\}$, $\{iiiAB\}$) are also listed in Table VII. It turns out that that this pair reveals much greater closeness than the original standardized sets.

Concerning other reasons for disparity between CFPs from various sources may include, as discussed in Refs. 8 and 15, e.g., the quality of the experimental energy levels, the validity of the assignments of the irreducible representations to the given states, or the correctness of the numerical procedures used to obtain the CFP datasets from fittings. In view of Burdick *et al.*'s^{26,36,37} intensity studies indicating a plethora of multiple local minima that fit the data nearly equally well, it is rather surprising that only single fitting results were reported in Refs. 16 and 18. It may be possible that the CFP datasets of Refs. 16 and 18 represent two different close-lying local minima. Repeating the fittings using the original experimental energy levels may help bring the resulting CFPs closer to each other. However, it should be kept in mind that even for a very well-studied system, namely, LiYF_4 doped with a number of R^{3+} ions, the CFPs even for the same ion reported by various authors reveal large disparities.³⁸

V. SUMMARY AND CONCLUSIONS

The present paper provides a thorough treatment of the intricacies concerning the properties of the crystal-field Hamiltonians for transition ions at orthorhombic and monoclinic symmetry sites. The CF Hamiltonian H_{CF} together with the free-ion terms underlie theoretical interpretation of experimental data obtained, e.g., optical spectroscopy, inelastic neutron scattering, and magnetic susceptibility measurements. Moreover, the intricate properties in question apply also to the zero-field-splitting Hamiltonians, which are the cornerstone of EMR studies. Hence, our considerations have wide implications in various areas.

The CF parameters for the Nd^{3+} ion in $\text{Nd}_2\text{BaCuO}_5$ obtained by R. S. Puche *et al.*¹⁶ from simple overlap model calculations and those fitted from the experimental data turn

out to be not directly compatible with the CFPs from other authors, criticized by them. We have reanalyzed the CFPs of Ref. 16 and those determined for the Nd^{3+} ion in $\text{Nd}_2\text{BaCuO}_5$ and $\text{Nd}_2\text{Ba}(\text{Zn}, \text{Cu})\text{O}_5$ from the absorption spectra by Klimin *et al.*¹⁸ and the experimental CFPs of Taibi *et al.*³³ for the Nd^{3+} ion in $\text{Nd}_2\text{BaZnO}_5$, which were used as the initial ones for fittings in Ref. 18. Our considerations are based on application of the standardization idea as well as the idea of dataset closeness, which enables their quantitative assessment using the closeness factors C and the norms ratios $R=N_A/N_B$ for the respective H_{CF} terms, $k=2, 4, 6$, and the global ones C_{gl} . Reanalysis of the experimental and/or theoretical nonstandard datasets for the ion-host system under investigation removes their incompatibility and makes the compatible CFPs numerically closer concerning most of the closeness quantities. Such well-quantified closeness may be contrasted favorably with the apparent results of a direct comparison of the incompatible CFP sets belonging to different regions of the parameter space done by some authors. In fact, direct comparisons in such cases turn out to be meaningless.

This study has enabled clarification of the controversy arising when comparing the standard CF parameters with the nonstandard CFPs evident in the R. S. Puche *et al.*¹⁶ study. It turns out that their criticism of the data of Klimin *et al.*¹⁸ and, by implication, of Taibi *et al.*³³ is unjustified. The controversy in question originates from the lack of awareness of the standardization idea applicable to the orthorhombic (as well as monoclinic and triclinic) CFP datasets. Another important result is the determination of the alternative physically equivalent CFP datasets generated by the standardization transformations. These CFP datasets have been utilized in the multiple correlated fitting technique. A number of re-fittings of the original energy level data¹⁸ were carried out starting from six distinct regions in the multiparameter space. The independently fitted nonstandard CFPs obtained in this way were then transformed to the standard region and inter-correlated. Averaging over the total number of the inter-correlated sets (here 18) obtained from the MCFT as well as over the two types of CFP sets (A and B) enables increasing substantially the reliability of the determination of the final CFPs. Considerations of the standardization and the dataset closeness have also helped in identifying other inconsistencies concerning the results.¹⁶ Structural implications of our crystal-field analysis and the inconsistencies in question have also been discussed. Our findings call for reconsideration of the theoretical and experimental data of R. S. Puche *et al.*¹⁶ along the lines proposed above. We suggest repeating the CFP fittings using the MCFT and the systematic procedures presented in Secs. III and IV.

Our literature survey indicates a rather low level of awareness of standardization and its usefulness among the optical spectroscopy practitioners. It may be hoped that this paper helps to improve the general awareness in future studies. A comparative analysis, along the lines worked out in this study, of the available CFPs for various trivalent rare earth R^{3+} ions,^{39–45} e.g., Nd, Er, and Eu, in the series of crystals $R_2\text{BaXO}_5$ ($X=\text{Cu}, \text{Zn}, \text{Ni}, \text{and Co}$), as well as Eu dopant ions in Y_2BaZnO_5 and $\text{La}_2\text{BaZnO}_5$ crystals, is now in progress. Such studies may enable us to solve similar con-

troversies and improve the understanding of the intricacies inherent in low-symmetry CFP datasets. It may be expected that this series of papers may help in reducing the confusion concerning the not-to-well-understood properties of low-symmetry CF Hamiltonians, still proliferating in various ways in the literature.

ACKNOWLEDGMENTS

This work was partially supported by a research grant from the Polish Ministry of Science and Tertiary Education (2006–2009). The authors are grateful to M. Reid for providing us with the fitting program. P.G. acknowledges gratefully financial support from the Institute of Physics, SUT.

*Corresponding author. crudowicz@ps.pl

†Present address: Faculty of Chemistry, University of Wrocław, ul. F. Joliot-Curie 14, 50–383 Wrocław, Poland.

- ¹C. Rudowicz and R. Bramley, *J. Chem. Phys.* **83**, 5192 (1985).
- ²C. Rudowicz, *J. Chem. Phys.* **84**, 5045 (1986).
- ³A. Abragam and B. Bleaney, *Electron Paramagnetic Resonance of Transition Ions* (Dover, New York, 1986).
- ⁴S. Altshuler and B. M. Kozyrev, *Electron Paramagnetic Resonance in Compounds of Transition Elements* (Wiley, New York, 1974).
- ⁵J. R. Pilbrow, *Transition-Ion Electron Paramagnetic Resonance* (Clarendon Press, Oxford, 1990).
- ⁶F. E. Mabbs and D. Collison, *Electron Paramagnetic Resonance of d Transition-Metal Compounds* (Elsevier, Amsterdam, 1992).
- ⁷C. Rudowicz and S. B. Madhu, *J. Phys.: Condens. Matter* **11**, 273 (1999).
- ⁸C. Rudowicz and S. B. Madhu, *Physica B* **279**, 302 (2000).
- ⁹D. Newman and B. Ng, *Crystal Field Handbook* (Cambridge University Press, Cambridge, U.K., 2000).
- ¹⁰B. Henderson and R. H. Bartram, *Crystal-Field Engineering of Solid-State Laser Materials* (Cambridge University Press, Cambridge, U.K., 2000).
- ¹¹J. Mulak and Z. Gajek, *The Effective Crystal Field Potential* (Elsevier, Amsterdam, 2000).
- ¹²M. Wildner, M. Andrut, and C. Rudowicz, in *Spectroscopic Methods in Mineralogy*, European Mineralogical Union Notes in Mineralogy, edited by A. Beran and L. Libowitzky (Eötvös University Press, Budapest, 2004), Vol. 6, Ch. 3.
- ¹³C. Rudowicz, M. Chua, and M. F. Reid, *Physica B* **291**, 327 (2000).
- ¹⁴C. Rudowicz and J. Qin, *J. Lumin.* **110**, 39 (2004).
- ¹⁵C. Rudowicz and J. Qin, *J. Alloys Compd.* **389**, 256 (2005).
- ¹⁶R. S. Puche, E. Climent, J. Romero de Paz, J. L. Martínez, M. A. Monge, and C. Cascales, *Phys. Rev. B* **71**, 024403 (2005).
- ¹⁷P. Porcher, Computer code REEL (1989).
- ¹⁸S. A. Klimin, M. N. Popova, E. Antic-Fidancev, and P. Porcher, *J. Solid State Chem.* **162**, 42 (2001).
- ¹⁹C. Rudowicz, *J. Phys. C* **18**, 1415 (1985); **18**, 3837 (1985).
- ²⁰C. Rudowicz, *Magn. Reson. Rev.* **13**, 1 (1987); **13**, 335 (1988).
- ²¹C. Rudowicz and C. Y. Chung, *J. Phys.: Condens. Matter* **16**, 5825 (2004).
- ²²C. Rudowicz and S. K. Misra, *Appl. Spectrosc. Rev.* **36**, 11

- (2001).
- ²³C. Rudowicz and J. Qin, *Phys. Rev. B* **67**, 174420 (2003).
- ²⁴C. Rudowicz and J. Qin, *Physica B* **364**, 239 (2005).
- ²⁵C. Rudowicz and P. Gnutek, *J. Alloys Compd.* doi:10.1016/j.jallcom.2007.02.088 (2007).
- ²⁶G. W. Burdick and M. F. Reid, *Mol. Phys.* **102**, 1141 (2004).
- ²⁷C. Rudowicz and P. Gnutek, (unpublished).
- ²⁸C. Rudowicz, in *Crystal Field Handbook*, edited by D. J. Newman and B. Ng (Cambridge University Press, Cambridge, U.K., 2000), p. 259.
- ²⁹C. Rudowicz and Q. Jian, *Comput. Chem. (Oxford)* **26**, 149 (2002).
- ³⁰K. W. H. Stevens, *Magnetic Ions in Crystals* (Princeton University Press, Princeton, NJ, 1997).
- ³¹C. Rudowicz and H. W. F. Sung, *Physica B* **300**, 1 (2001).
- ³²C. Rudowicz, *J. Phys.: Condens. Matter* **12**, L417 (2000).
- ³³M. Taibi, J. Aride, E. Antic-Fidancev, M. Lemaitre-Blaise, and P. Porcher, *Phys. Status Solidi A* **115**, 523 (1989).
- ³⁴C. Rudowicz, *Chem. Phys.* **97**, 43 (1985).
- ³⁵P. Porcher, M. C. Dos Santos, and O. Malta, *Phys. Chem. Chem. Phys.* **1**, 397 (1999).
- ³⁶G. W. Burdick, R. L. Summerscales, S. M. Crooks, M. F. Reid, and F. S. Richardson, *J. Alloys Compd.* **301-304**, 376 (2000).
- ³⁷G. W. Burdick, E. S. LaBianca, and D. L. Binus, *J. Alloys Compd.* **344**, 327 (2002).
- ³⁸C. Rudowicz and Q. Jian, *J. Alloys Compd.* **385**, 238 (2004).
- ³⁹M. N. Popova, S. A. Klimin, E. P. Chukalina, E. A. Romanov, B. Z. Malkin, E. Antic-Fidancev, B. V. Mill, and G. Dhalenne, *Phys. Rev. B* **71**, 024414 (2005).
- ⁴⁰M. N. Popova, S. A. Klimin, E. P. Chukalina, B. Z. Malkin, R. Z. Levitin, B. V. Mill, and E. Antic-Fidancev, *Phys. Rev. B* **68**, 155103 (2003).
- ⁴¹S. Taboada, A. de Andres, J. E. Munoz Santiuste, C. Prieto, J. L. Martinez, and A. Criado, *Phys. Rev. B* **50**, 9157 (1994).
- ⁴²S. Taboada, A. de Andres, and J. E. Munoz-Santiuste, *J. Phys.: Condens. Matter* **10**, 8983 (1998).
- ⁴³S. Taboada, A. de Andres, and R. S. Puche, *J. Alloys Compd.* **275-277**, 279 (1998).
- ⁴⁴M. N. Popova, S. A. Klimin, E. Antic-Fidancev, P. Porcher, M. Taibi, and J. Aride, *J. Alloys Compd.* **284**, 138 (1999).
- ⁴⁵S. J. Harker, G. A. Stewart, and P. C. M. Gubbens, *J. Alloys Compd.* **307**, 70 (2000).